Life Sciences 218 (2019) 265–273

Contents lists available at ScienceDirect

Life Sciences

journal homepage: www.elsevier.com/locate/lifescie

The appropriate remodeling of extracellular matrix is the key molecular signature in subcutaneous adipose tissue following Roux-en-Y gastric bypass

Xiangjun Chen[a], Lilin Gong[a], Qifu Li[a], Jinbo Hu[a], Xiurong Liu[a], Yao Wang[a], Jie Bai[a], Xi Ran[a], Jinshan Wu[a], Qian Ge[a], Rong Li[a], Xiaoqiu Xiao[a,b], Xi Li[c], Jun Zhang[d], Zhihong Wang[a,*]

[a] Department of Endocrinology, The First Affiliated Hospital of Chongqing Medical University, Chongqing, China
[b] Laboratory of Lipid and Glucose Metabolism, The First Affiliated Hospital of Chongqing Medical University, Chongqing, China
[c] Biology Science Institutes, Chongqing Medical University, Chongqing, China
[d] Department of Gastrointestinal Surgery, The First Affiliated Hospital of Chongqing Medical University, Chongqing, China

ARTICLE INFO

Keywords:
Roux-en-Y gastric bypass
Subcutaneous adipose tissue
Extracellular matrix remodeling
Transcriptomics
Bioinformatics

ABSTRACT

Aims: We sought to reveal the key molecular signature in subcutaneous adipose tissue (scAT) following Roux-en-Y gastric bypass (RYGB), through bioinformatics analysis and further verification in vivo.

Main methods: We obtained a transcriptome data of scAT from RYGB and sham-operated rats from the Gene Expression Omnibus. The differentially expressed genes (DEGs) were screened and the DEGs-related Gene ontology (GO) functions and Kyoto Encyclopedia of Genes and Genomes (KEGG) pathways were analyzed. Also, the protein-protein interaction (PPI) network was constructed among the DEGs. Furthermore, we established an experimental rat model to verify the bioinformatics findings.

Key findings: Using the method of bioinformatics, a total of 602 genes were found to be differentially expressed in scAT between the RYGB group and the sham-operated group. GO analysis showed that DEGs were significantly enriched in extracellular matrix(ECM) -associated functions or processes. KEGG pathway analysis revealed that the protein digestion and absorption pathway and ECM-receptor interaction pathway were the most significantly enriched pathways. The genes encoding ECM components and ECM remodeling-related proteins interact substantially in the PPI network. Then the results of rat experimental verified that the gene expression levels of ECM components(Collagen I and III) and ECM cross-linking related proteins(lysyl oxidase and lysyl oxidase-like 1) decreased and ECM dagradation-related proteins increased in scAT following RYGB. These beneficial results were positively associated with improved insulin resistance (IR).

Significance: Appropriate ECM remodeling, primarily the reduction of ECM deposition and cross-linking and the increase of ECM dagradation, may be the key molecular signature in scAT following RYGB.

1. Introduction

The growing incidence of obesity is widely recognized as one of the most challenging threats to public health [1]. Obesity is implicated as a cause of many chronic metabolic diseases, including diabetes, hypertention, dyslipidemia and cardiovascular disorders [2]. Bariatric surgeries, including Roux-en-Y gastric bypass (RYGB), are considered to be the most effective strategies for obesity. Not only do these types of surgeries produce significant weight loss, but also improve associated insulin resistance (IR) and whole body metabolic function [3,4].

Following significant weight loss after bariatric surgery, the morphology and function of adipose tissue undergo substantial changes, mainly manifested by the reduction of size of both adipocytes [5,6] and individual depots [7,8], the alternation of adipose tissue secretory profile [9–16], the alleviation of chronic low-grade inflammation [17–21] and IR [22–25]. However, the major functions and pathways that are modified in adipose tissue in response to bariatric surgery are not fully understood. The study of omics, such as transcriptomics, proteomics or metabolomics, could provide a more complete picture than the study of single gene to understand the major mechanism of disease. The subsequent bioinformatics analysis is used to interpret the biological data produced by omics.

To investigate the changes of gene expression in adipose tissue after bariatric surgery, the transcriptomics have been recently studied by several researchers [26–28]. Using the before and after design, Liu and Henegar examined the changes of transcriptomes in subcutaneous

* Corresponding author at: Department of Endocrinology, Chongqing Medical University, Youyi Street Yuanjiagang, Yuzhong District, Chongqing, China.
E-mail address: towzh713@126.com (Z. Wang).

https://doi.org/10.1016/j.lfs.2018.12.051
Received 3 October 2018; Received in revised form 24 December 2018; Accepted 29 December 2018
Available online 31 December 2018

adipose tissue (scAT) from obese patients before and after bariatric surgery [26,27]. Cancello et al. compared the scAT transcriptomes of ex-obese patients who had a stable weight for at least 2 years with the transcriptomes of obese patients [28]. It is worth noting that the scAT gene expression profiles of aformentioned transcriptome studies are inconsistent. Liu and Henegar's transcriptome study were before and after studies, which may affected by some irrelevant variables, such as time factor and environment change [29]. Cancello' study may have a selective bias of research subjects because the samples have not been comparable in their demography and characteristics. The inclusion of a sham treatment, as a control group which had the similar characteristics to the intervention group could effectively control the confounding factors and possible selective bias in above studies performed on humans. However, the use of sham treatments in human research is ethically controversial.

Transcriptome data for comparing the gene expression of scAT between obese rats underwent RYGB and obese rats underwent sham operation and pair fed as RYGB group was provided by Guijarro et al. The intervention group and sham treatment group were studied concurrently would effectively control possible influences of irrelevant variables on scAT transcriptome. Guijarro' study focused on energy related transcripts associated with RYGB and they did not interpret the transcriptome data at bioinformatics perspectives. So, in current study, this transcriptome data was used for systematic bioinformatics analyses to discuss the major functions and signaling pathways involved in scAT following RYGB. Furthermore, we verified the bioinformatics findings in our rat experimental. The current study may reveal the key molecular signature in scAT following RYGB and provide a more comprehensive understanding on the involvement of adipose tissue in metabolic dysfunction improvement by bariatric surgery.

2. Materials and methods

2.1. Data acquisition and preprocessing

The transcriptome data for subcutaneous abdominal fat from obese rats underwent RYGB for 3 months(RYGB group, n = 3) and obese rats underwent sham operation, pair fed as those in RYGB (Sham group, n = 3), have been deposited in the database of GEO (Accession no. GSE8314) [30]. We downloaded the raw Affymetrix CEL files based on the platform of Affymetrix Rat Genome 230 2.0 Array. The raw data underwent pre-processing, including background correction, quantile normalization and probe summarization with the application of bioconductor package 'affy', as previousy described [31].

2.2. Analysis of DEGs

The DEGs in the RYGB group compared with the sham group were analyzed using the Bioconductor package 'limma', as previously described [32]. The p-value for each gene was calculated using the Student's *t*-test. Genes with differences in expression denoted by values of p-value < 0.05 and $|\log2FC \text{ (fold change)}| \geq 1$, screened as DEGs. In order to compare the differences in the profiles of DEGs between the RYGB and control samples, the gene expression data were clustered using R 'pheatmap' software package (https://cran.r-project.org/web/packages/pheatmap/index.html).

2.3. GO analysis and KEGG pathway analysis

The upregulated and downregulated genes were subjected to GO and KEGG pathway analysis. The GO analysis contains terms under the three categories: cellular component(CC), molecular function(MF), and biological process(BP). GO and KEGG pathway enrichment analyses were performed using the Database for Annotation, Visualization and Integrated Discovery (DAVID, http://david.abcc.ncifcrf.gov/) online tool. The cut-off value for a significant GO term and pathway was set to p-value < 0.05 and count ≥ 2.

2.4. Construction of PPI network

The Retrieval of Interacting Genes (STRING) database tool (https://string-db.org/) was used to evaluate the interactive relationships among the DEGs. The PPI score was set as 0.4 and other parameters were set as the default value. Cytoscape was used to visualize the PPI network. Subsequently, with the application of CytoNCA [33], the hub nodes were measured based on the degree centrality [34], betweenness centrality [35] and subgraph centrality [36].

2.5. Animal model

All animal studies were approved by the Ethics Committee of Chongqing Medical University and all experiments were performed in accordance with relevant guidelines and regulations. Male Sprague-Dawley rats (4 weeks old, the Animal Center of Chongqing Medical University, Chongqing, China) were kept under a 12-h light/12-h dark cycle at a constant temperature of 23 ± 2 °C. After 1 week of acclimatization, 12 rats were given a Western high-fat diet (HFD) with 45% of kcal derived from fat (#D12451; 4.73 kcal/g, 45% from fat; Research Diets, New Brunswick, NJ, USA) and 6 rats were given a normal chow diet (NCD) (#D12450B; 3.85 kcal/g, 10% from fat; Research Diets) as the control. The methods of evaluation body weight, body fat mass, fasting blood glucose and fasting insulin were shown in our previous study [37].

2.6. Surgery process and postsurgical management

After the rats were fed an HFD for 16 weeks, the rats were randomly divided into two groups: sham group(sham operation on HFD induced obesity rats, n = 6) and RYGB group(RYGB operation on HFD induced obesity rats, n = 6). While the NCD groups did not receive surgical intervention, the details of the process of operation was shown in our previous study [37,38]. After surgery, animals were housed individually and fasted for 24 h. Then the animals were allowed to eat a liquid diet and had access to water ad libitum for 2 days. At the 4th day, animals were allowed to eat regular chow. Six weeks after surgery, we acquired blood samples for measuring fasting blood glucose and fasting insulin, then homeostasis model assessment of insulin resistance (HOMA-IR) were also calculated [39]. Eight weeks after surgery, all rats were sacrificed and the scAT were collected and stored at −80 °C or fixed in 4% formaldehyde.

2.7. Masson's Trichrome staining and quantitative RT-PCR

To assess morphological and fibrotic changes, Masson's Trichrome staining was performed in 5-μm thick cross sections of fat tissues. Following deparaffinization and rehydration, tissue sections were stained by Masson Stain Kit(D026,Nanjing,China). Total RNA was extracted from frozen scAT samples using the Trizol reagent (TaKaRa, Kusatsu, Japan) and complementary DNA (cDNA) was synthesized by reverse transcription using the EvoScript Universal cDNA Master (Roche Diagnostics, Mannheim, Germany). Quantitative real-time polymerase chain reaction (RT-PCR) analysis was performed with One Step SYBR Green (Roche Diagnostics, Mannheim, Germany) in a RT-PCR apparatus (Bio-rad, CA, USA). The delta-delta Ct method was used to determine the fold change for each group, with the International Standard Organization (ISO) group as reference. Primer sequences (Supplementary Table 1) were designed using Primer-BLAST (www.ncbi.nlm.nih.gov/tools/primer-blast/).

2.8. Statistical analysis

SPSS Statistics 22.0 was used to conduct all statistical analyses. Data

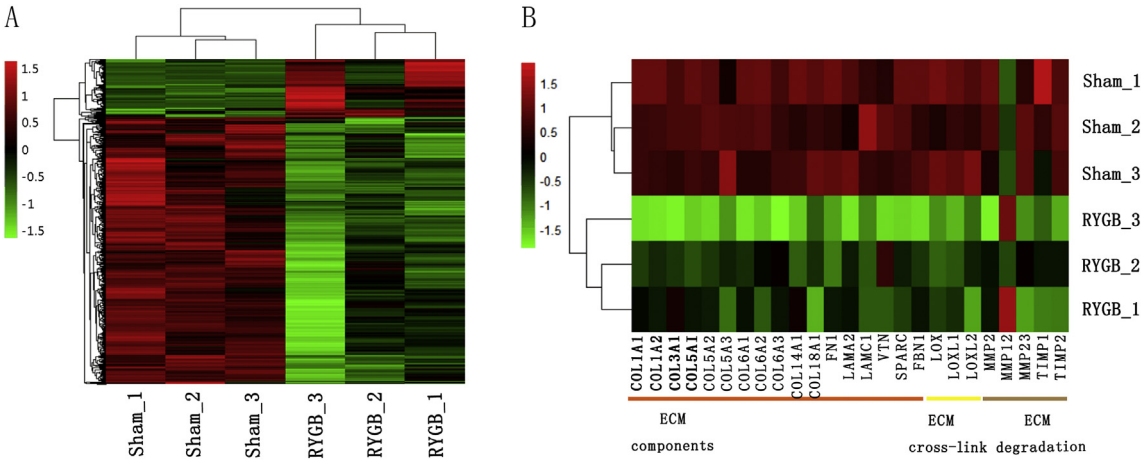

Fig. 1. A.The heatmap of gene expression profiles of DEGs between RYGB and Sham group. Green, low gene expression value; red, high gene expression value; black, no differential expression. RYGB group, who have underwent RYGB for 3 months (n = 3); Sham group who underwent sham operation and were pair fed as RYGB (n = 3). Abbreviations: DEGs, differentially expressed genes; RYGB, Roux-en-Y gastric bypass. B.The heatmap of gene expression profiles of genes encoding ECM between RYGB and Sham group. Green, low gene expression value; red, high gene expression value; black, no differential expression. RYGB group, who have underwent RYGB for 3 months (n = 3); Sham group who underwent sham operation and were pair fed as RYGB (n = 3). Abbreviations: ECM, Extracellular matrix; RYGB, Roux-en-Y gastric bypass; COL1A1, Collagen type I alpha 1 chain; COL1A2, Collagen type I alpha 2 chain; COL3A1, Collagen type III alpha 1 chain; COL5A1, Collagen type V alpha 1 chain; COL5A2, Collagen type V alpha 2 chain; COL5A3, Collagen type V alpha 3 chain; COL6A1, Collagen type VI alpha 1 chain; COL6A2, Collagen type VI alpha 2 chain; COL6A3, Collagen type VI alpha 3 chain; COL14A1, Collagen type XIV alpha 1 chain; COL18A1, Collagen type XVIII alpha 1 chain; FN1, Fibronectin 1; LAMA2, Laminin, alpha 2; LAMC1, Laminin, gamma 1; VTN, vitronectin; Sparc, Secreted protein acidic and cysteine rich; FBN1, Fibrillin 1; LOX, Lysyl oxidase; LOXL1, Lysyl oxidase-like 1; LOXL2, Lysyl oxidase-like 2; MMP2, Matrix metallopeptidase 2; MMP12, Matrix metallopeptidase 12; MMP23, Matrix metallopeptidase 23; TIMP1, Tissue inhibitor of metalloproteases 1; TIMP2, Tissue inhibitor of metalloproteases 2. (For interpretation of the references to colour in this figure legend, the reader is referred to the web version of this article.)

are presented as the means ± standard error (S.E.M). Nonparametric test was performed to determine differences among > 2 groups. Pearson correlation was also calculated to evaluate the relationship between reduced HOMA-IR and changed expression of ECM. $P < 0.05$ was considered statistically significant. Significance is shown as * $p < 0.05$, ** $p < 0.01$ or *** $p < 0.001$.

3. Results

3.1. Identification of DEGs

After preprocessing, the gene expression data were normalized (Supplementary Fig. 1). According to values of p-value < 0.05 and $|\log_2 FC(\text{fold change})| \geq 1$, a total of 602 genes were found to be differentially expressed between the RYGB group and the sham group, including 494 down-regulated and 108 up-regulated genes. The information on the top 50 genes which were down-regulated ("Supplementary Table 2") or up-regulated ("Supplementary Table 3") between the RYGB group and the sham group were provided. The up-regulated and down-regulated genes were relatively distinguished between the two groups by hierarchical clustering analysis (Fig. 1A).

3.2. Enrichment analysis of DEGs

To further explore the key biological functions and pathways associated with DEGs in RYGB group, we used unbiased pathway analyses including GO functional annotation and KEGG pathway enrichment analysis. Three GO categories, including BP, CC and MF, were selected in the functional annotation.

The top five GO terms for DEGs were listed in Table 1, including collagen fibril organization, extracellular matrix organization in the BP category, extracellular matrix and extracellular space in the CC category, extracellular matrix structural constituent and extracellular matrix binding in the MF category. Of note, among the significantly enriched GO terms, several pointed towards ECM-associated functions or processes.

Table 1
The significant GO terms enriched by DEGs.

Term	Count	p Value
BP		
GO:0030199~collagen fibril organization	12	7.56E-09
GO:0007156~homophilic cell adhesion via plasma membrane adhesion molecules	19	1.92E-07
GO:0030198~extracellular matrix organization	15	4.58E-07
GO:0042060~wound healing	16	2.22E-06
GO:0006508~proteolysis	33	3.39E-06
CC		
GO:0031012~extracellular matrix	56	2.73E-33
GO:0005615~extracellular space	119	4.46E-31
GO:0070062~extracellular exosome	174	2.41E-29
GO:0005578~proteinaceous extracellular matrix	50	2.17E-27
GO:0005604~basement membrane	19	8.04E-11
MF		
GO:0005509~calcium ion binding	61	4.73E-15
GO:0008201~heparin binding	25	2.11E-12
GO:0005201~extracellular matrix structural constituent	11	4.17E-07
GO:0050840~extracellular matrix binding	8	6.73E-06
GO:0005518~collagen binding	11	7.39E-06

Abbreviations: GO, Gene ontology; DEGs, Differentially expressed genes; BP, Biological process; CC, Cellular component; MF, Molecular function.

DEGs were found to be significantly enriched in 22 KEGG pathways (Table 2). Protein digestion and absorption pathway (p-value = 8.34E-10) and ECM-receptor interaction pathway(p-value = 5.02E-08) were the most significantly enriched pathways. Other pathways, such as Complement and coagulation cascades, PI3K-Akt signaling pathway and Focal adhesion were significantly enriched by DEGs.

3.3. The expression profiles of genes encoding ECM components and ECM remodeling-related proteins

ECM is a collection of extracellular molecules, including collagen, non-collagen proteoglycan, proteoglycan and proteins that regulate the synthesis, degradation and cross-linking of ECM. When the proteins

Table 2
KEGG pathways significantly enriched by DEGs.

Term	Count	p Value
rno04974:Protein digestion and absorption	18	8.34E-10
rno04512:ECM-receptor interaction	16	5.02E-08
rno04610:Complement and coagulation cascades	13	1.29E-06
rno04151:PI3K-Akt signaling pathway	27	9.45E-06
rno04510:Focal adhesion	20	1.67E-05
rno00480:Glutathione metabolism	10	5.08E-05
rno05150:Staphylococcus aureus infection	9	1.87E-04
rno05146:Amoebiasis	12	5.20E-04
rno00980:Metabolism of xenobiotics by cytochrome P450	9	0.001122613
rno04640:Hematopoietic cell lineage	9	0.002882998
rno04142:Lysosome	11	0.004819169
rno00982:Drug metabolism - cytochrome P450	8	0.005270345
rno05204:Chemical carcinogenesis	9	0.00589711
rno05205:Proteoglycans in cancer	14	0.0074979
rno00520:Amino sugar and nucleotide sugar metabolism	6	0.014097271
rno05020:Prion diseases	5	0.014808183
rno04614:Renin-angiotensin system	5	0.014808183
rno05133:Pertussis	7	0.022109685
rno05143:African trypanosomiasis	5	0.026444441
rno05144:Malaria	6	0.031655994
rno04925:Aldosterone synthesis and secretion	7	0.040339991
rno05031:Amphetamine addiction	6	0.042796421

Abbreviations: DEGs, Differentially expressed genes.

regulating ECM synthesis, degradation and cross-linking are unbalanced, the ECM remodeling occurs.

We explore whether the expression of genes encoding ECM component and ECM remodeling-related proteins changed in scAT following RYGB. As shown in Fig. 1B, the genes encoding ECM components, such as collagen I(COL1A1, COL1A2), collagen III (COL3A1), collagen V(COL5A1, COL5A2, COL5A3), collagen VI(COL6A1, COL6A2), and fibronectin(FN1) were significantly down-regulated in RYGB group compared with the sham group. The genes encoding matrix metalloproteinases (MMPs) and tissue inhibitor of metalloproteinases(TIMPs), responsible for the degradation of virtually all ECM proteins, were found to be differentially expressed. Finally, we observed a significant down-regulation of genes encoding cross-linking enzymes such as lysyl oxidase(LOX), lysyl oxidase-like 1(LOXL1), lysyl oxidase-like 2(LOXL2) in the RYGB group.

3.4. The genes encoding ECM components and ECM remodeling-related proteins interact a lot in PPI network

It has been widely acknowledged that proteins rarely act alone, but interact with each other. By uploading the DEGs into the PPI network tool, we found 89 nodes and 139 edges in the PPI network (Fig. 2). The red nodes indicated the genes encoding ECM components, and the yellow nodes indicated ECM remodeling-related proteins, such as LOX, MMPs and other cytokines. The blue nodes indicated genes encoding other proteins. We discovered that the genes encoding ECM components and the genes encoding ECM remodeling-related proteins interact a lot in this PPI network.

Usually, the genes with higher degree are known as significant genes or hub genes. By the method of 'cytoNCA', we identified the top 15 hub genes between the RYGB group and the sham group (Table 3). Most of them are associated with ECM, such as secreted protein acidic and cysteine rich(SPARC), collagen V, decorin and LOX.

3.5. Validation of bioinformatic findings by experimental rat model

Our above bioinformatics analyses found the altered genes in scAT following RYGB were significantly enriched in ECM-associated functions or pathways. We subsequently explored the alteration of ECM in scAT following RYGB in our experimental rat model. As shown in our previous study [37], at 6 weeks after RYGB, there were significant reductions in body weight, body fat mass, fasting insulin and improvement of IR based on HOMA-IR evaluation, compared to the sham group.

We analyzed the alteration of ECM in rat subcutaneous fat 8 weeks after RYGB. Masson's Trichrome staining showed the fibrotic structural characteristics in scAT of the three groups. The collagen deposition in the sham group was markedly increased compared with that in rats of NCD group, while it decreased in RYGB group (Fig. 3A). The mRNA levels of COL1A2 (Fig. 3B) and COL3A1 (Fig. 3C) in the sham group significantly increased compared with NCD group, whereas it decreased in RYGB rats. No significant differences were noted between the sham group and RYGB group in terms of the mRNA levels of COL6A1 (Fig. 3D). The mRNA level of MMP2 (Fig. 3E) and MMP12 (Fig. 3F) in the sham group decreased compared with the NCD group, but it significantly increased in the RYGB group. The mRNA level of TIMP2 (Fig. 3G) in the sham group significantly increased compared with NCD group, it had a decreased trend in RYGB group. The gene expression levels of LOX (Fig. 3H) and LOXL1 (Fig. 3I) in the sham group significantly increased compared with NCD group, whereas it decreased in RYGB group.

Previous studies have found that excess ECM deposition in the adipose tissue deteriorates insulin sensitivity [40–43]. However, it is not clear whether the improved ECM remodeling following RYGB was associated with improved IR. We further made the correlation analysis between the changed level of ECM-related gene expression induced by RYGB and the reduced level of HOMA-IR induced by RYGB. The reduced expression level of COL3A1 ($r = 0.896$, p-value = 0.016), LOX ($r = 0.835$, p-value = 0.039) or LOXL1 ($r = 0.881$, p-value = 0.020) induced by RYGB were positively correlated with reduced HOMA-IR level. There is no correlation between changed expression level of COL1A2 ($r = 0.789$, p-value = 0.062) or COL6A1 ($r = 0.665$, p-value = 0.149) and reduced HOMA-IR level. The increased expression level of MMP2 ($r = 0.886$, p-value = 0.019) induced by RYGB was positively correlated with reduced HOMA-IR level. There is no correlation between the changed MMP12 ($r = 0.803$, p-value = 0.054) or TIMP2 ($r = 0.569$, p-value = 0.239) and reduced HOMA-IR level.

4. Discussion

To control the possible influence of irrelevant variables on scAT transcriptome, the intervention group and sham treatment group who had the similar characteristics to the intervention group were studied concurrently in the current study. In order to construct a comprehensive map of scAT transcriptome in response to RYGB, an integrative bioinformatics approach was applied to identify the main functions and signaling pathways annotating DEGs. We found that appropriate ECM remodeling, primarily the reduction of ECM deposition and cross-linking and the increase of ECM degradation, may be the key molecular signature in scAT following RYGB. Furthermore, we validated the bioinformatics findings in the rat experimental. The results of our validation experiments were mostly consistent with our bioinformatics findings.

With a similar bioinformatics approach, the transcriptome of scAT samples from five obese patients before and three months after bariatric surgery was analyzed by Henegar et al. [27]. Their study reported that several genes modified in scAT after bariatric surgery were associated with ECM related functions and pathways by GO and KEGG analyses [27]. Caution is needed when interpreting the results of the above before and after study. Over time, the function of ECM in adipose tissue becomes defective and an excessive accumulation of ECM components is described in adipose tissue [44–46]. Besides, the surgical incision by bariatric surgery may stimulate scAT to a tissue repair status: the scAT would secrete some cytokines and increase the production of ECM to repair postsurgical wounds [47–49]. So, in addition to the role of bariatric surgery, the time factor and environment change in scAT could impact the transcriptome results. To control these possible confounding

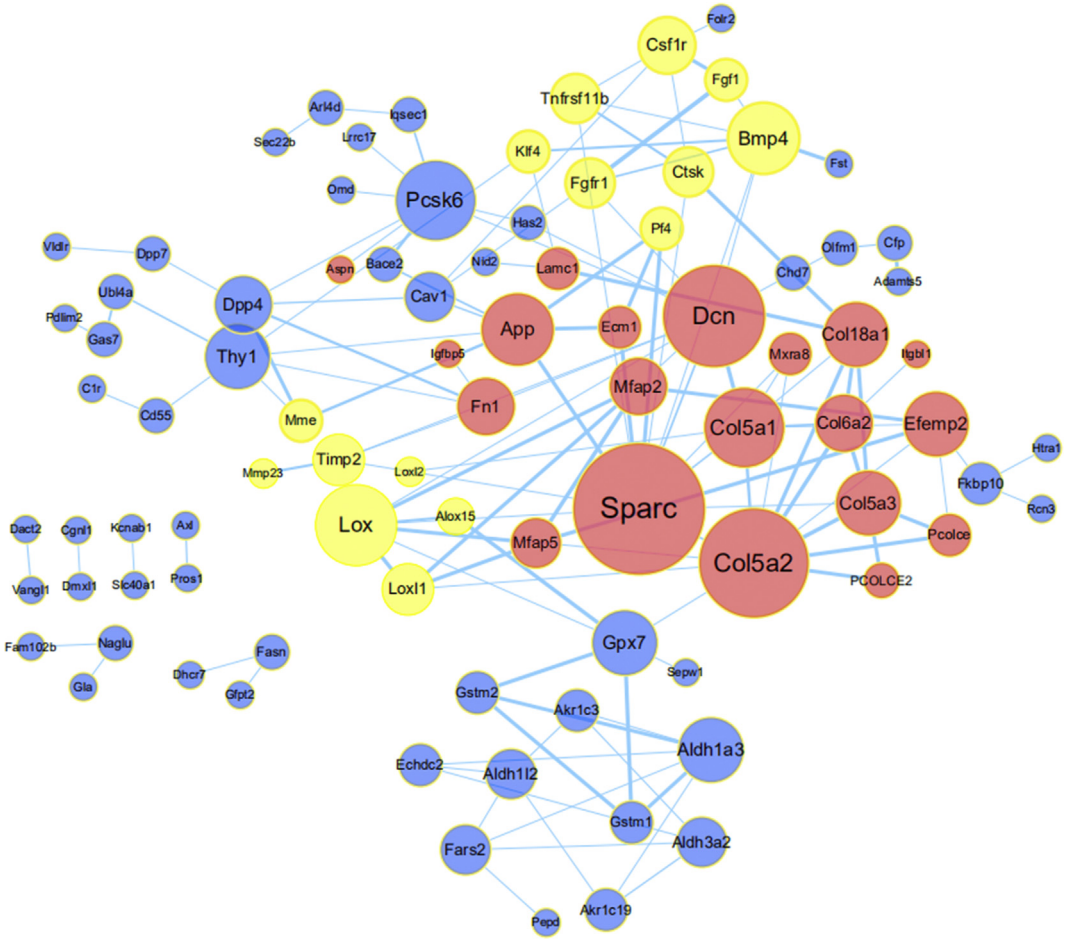

Fig. 2. Protein-protein interaction (PPI) network for DEGs. Every node in this network means one DEG, the size of the node based on the degree; every line in this network means one interaction between DEGs, the thickness of the line based on the strength of the interaction calculated by confidence score. Red nodes, genes encoding ECM components; yellow nodes, genes encoding ECM remodeling-related proteins; blue nodes, genes encoding other proteins. Abbreviations: DEGs, differentially expressed genes. (For interpretation of the references to colour in this figure legend, the reader is referred to the web version of this article.)

factors on scAT transcriptome, the RYGB group and sham-operated group, which had the similar characteristics to the RYGB group, were studied concurrently in the present study. Our bioinformatics analyses revealed that the most significantly enriched GO cellular component and GO biological process associated with the DEGs was "extracellular matrix" and "collagen fibril organization". The most significantly enriched KEGG pathways were "protein digestion and absorption" and "ECM-receptor interaction". Our transcriptome study pointed out the ECM alterations in scAT were the primary molecular signatures following RYGB.

Table 3
The top 15 significant nodes in the protein-protien interaction network based on degree.

Gene symbol	Degree	Subgragh	Eigenvector	LAC	Betweenness	Closeness	Network
Sparc	13	87.021385	0.39916018	2.15384630	1305.5381	0.060647830	6.6779222
Col5a2	12	83.826240	0.38581645	2.66666670	954.95240	0.059945505	7.7898270
Dcn	11	51.800550	0.28416288	1.45454550	2054.7620	0.060899653	3.8047620
Col5a1	8	48.528980	0.2954928	2.00000000	577.21906	0.060027286	3.3857143
Lox	8	44.073185	0.27073345	2.25000000	1086.0120	0.060232718	4.8166666
Pcsk6	8	12.896586	0.07527718	0.25000000	1007.5000	0.059020790	1.1428572
Bmp4	7	22.249138	0.16254023	1.14285720	400.67618	0.059339177	2.1666667
App	7	17.775747	0.12349646	1.14285720	603.06190	0.059339177	3.0333333
Col5a3	6	30.856140	0.22137396	2.00000000	101.38095	0.058981232	3.6000000
Col18a1	6	26.580000	0.19902547	1.66666660	255.93333	0.058823530	2.1500000
Efemp2	6	21.874159	0.1785573	1.00000000	463.73810	0.058316767	1.6833333
Gpx7	6	15.061400	0.12630615	1.00000000	1418.3334	0.058862876	2.6000000
Aldh1a3	6	9.4475040	0.009238202	0.33333334	944.00000	0.054692354	1.0000000
Thy1	6	8.9334190	0.048392072	0.33333334	774.96670	0.057932850	0.7000000
Col6a2	5	22.565060	0.18032587	2.00000000	147.00000	0.058278147	2.5000000

Abbreviations: Sparc, Secreted protein acidic and cysteine rich; Col5a2, Collagen type V alpha 2 chain; Dcn, Decorin; Col5a1, Collagen type V alpha 1 chain; Lox, Lysyl oxidase; Pcsk6, Proprotein convertase subtilisin/kexin type 6; Bmp4, Bone morphogenetic protein 4; App, Amyloid beta precursor protein; Col5a3, Collagen type V alpha 3 chain; Col18a1, Collagen type XVIII alpha 1 chain; Efemp2, EGF containing fibulin extracellular matrix protein 2; Gpx7, Glutathione peroxidase 7; Aldh1a3, Aldehyde dehydrogenase 1 family, member A3; Thy1, Thy-1 cell surface antigen; Col6a2, Collagen type VI alpha 2 chain.

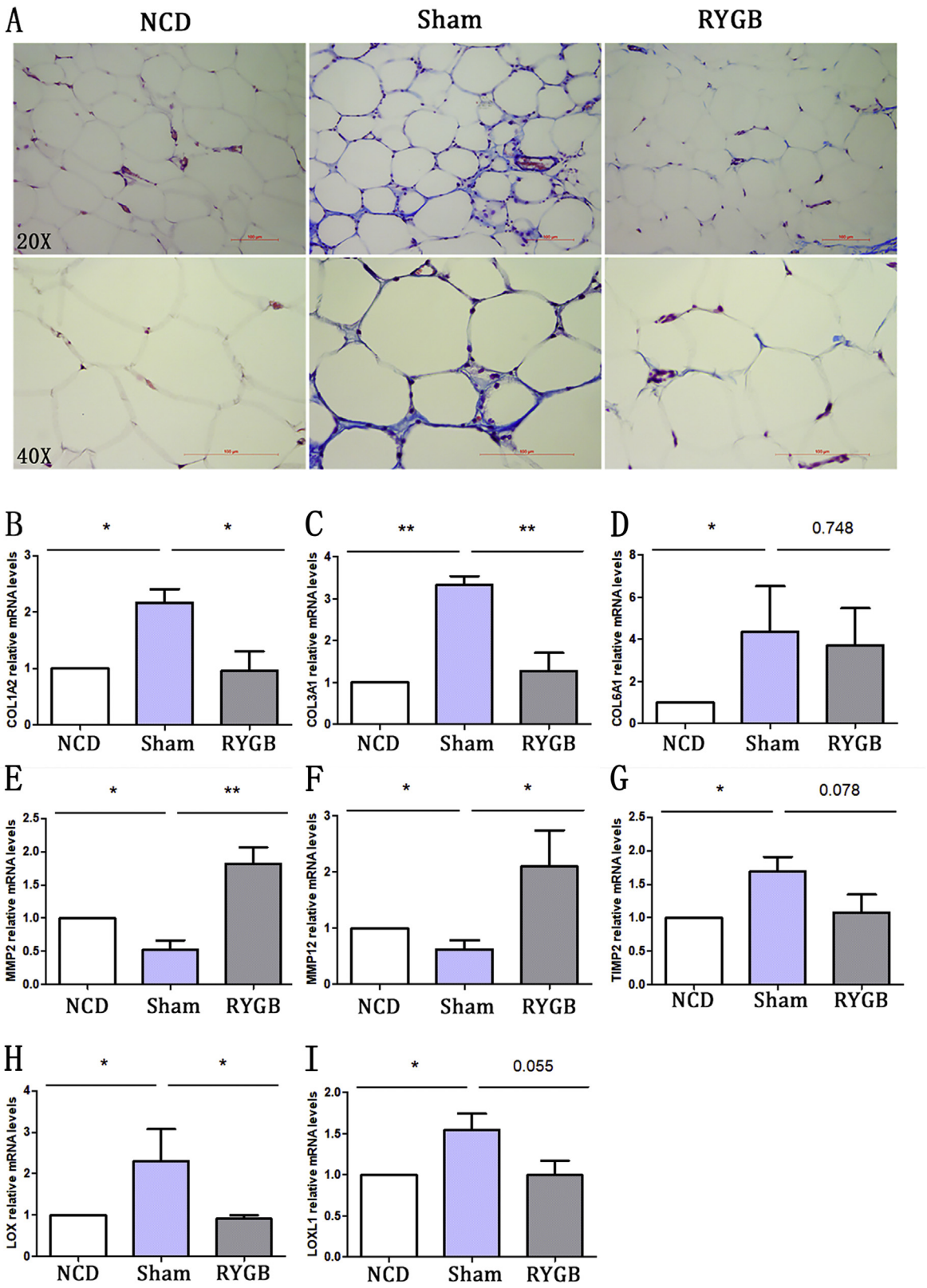

Fig. 3. A.Representative Masson's Trichrome staining of rat scAT among NCD, Sham and RYGB group. Collagen as blue, nuclei as black, and cytoplasm as red. Original magnification ×20 and ×40. B–H. The mRNA expression levels of the genes encoding COL1A2, COL3A1, COL6, MMP2, MMP9, TIMP2, LOX and LOXL1 of rat scAT among NCD, Sham and RYGB group. Data are presented as mean ± SEM. Significance is shown as * $p < 0.05$, ** $p < 0.01$. NCD group (n = 6), wo receive normal chow diet and without operation; Sham group (n = 6), sham operation on HFD induced obese rats for 8 weeks; RYGB group (n = 6), RYGB operation on HFD induced obese rats for 8 weeks. Abbreviations: scAT, subcutaneous adipose tissue; NCD, Normal chow diet; RYGB, Roux-en-Y gastric bypass; COL1A2, Collagen type I alpha 2 chain; COL3A1, Collagen type III alpha 1 chain; COL6A1, Collagen type VI alpha 1 chain; MMP2, Matrix metallopeptidase 2; MMP9, Matrix metallopeptidase 9; TIMP2, Tissue inhibitor of metalloproteases 2; LOX, Lysyl oxidase; LOXL1, Lysyl oxidase-like 1. (For interpretation of the references to colour in this figure legend, the reader is referred to the web version of this article.)

Based on the bioinformatics findings, we validated the ECM alterations in our experimental rat model. Masson's Trichrome staining showed that the collagen deposition in the RYGB group was markedly decreased compared to the sham group. Quantitative RT-PCR was used to examine the gene expression levels of ECM components and the molecules regulating ECM synthesis, cross-linking and degradation. We found that decreased collagen deposition and cross-linking of ECM and increased ECM degradation following RYGB. Our study is in accordance with Liu's study. Examining the alterations of ECM-related protein levels through immunohistochemistry before and one year after bariatric surgery, Liu's study showed that LOX and LOXL1 were down-regulated, collagen I and VI were down-regulated and degraded collagen I and III were increased after bariatric surgery, which suggested that decreased deposition and cross-linking of ECM and increased degradation of ECM after bariatric surgery [26]. However, similar findings were not found in other studies which focused on the ECM alterations in scAT following bariatric surgery. The scAT fibrosis(manifested as by excessive ECM deposition and cross-linking) levels was examined by picrosirius red staining in five obese patients before and three months after bariatric surgery by Henegar et al. They found no significant decrease of scAT fibrosis three months after bariatric surgery [27]. Chabot studied the scAT of 31 obese patients before and 6 months after bariatric surgery. They did not find any alterations of indicators for ECM(COL4A2, LOX, COL3A1, LAMB2 and COL6A3) in scAT 6 months after bariatric surgery by RT-PCR [50]. The defects of before and after study - neglecting the influences of time factor and environment change on the scAT transcriptome - may partially account for the inconsistency in human studies. Besides, the above studies with inconsistent results used different biopsy methods(perisurgical incisional biopsy, postoperative needle biopsy) to obtain scAT samples before and after surgery. Compared to the incisional biopsy, the needle-aspirated biopsy had little to no fibrotic regions by immunohistochemistry experiments confirmation [51].

ECM is a collection of extracellular molecules, including collagen, non-collagen proteoglycan, proteoglycan and proteins that regulate the synthesis, degradation and cross-linking of ECM. Disturbances of ECM homeostasis, leading to inappropriate remodeling of ECM, are known to be associated with a number of pathological conditions, such as cancer and fibrotic diseases [52–54]. The inappropriate ECM remodeling in AT, usually manifested as an excessive deposition of ECM components (mainly cross-linked collagens) and impaired degradation, is increasingly appreciated as a major hallmark of dysfunction AT in obesity [46,55]. On one hand, the inappropriate ECM remodeling reduces adipose tissue plasticity and results in ectopic fat storage and metabolic disorders [40–43]. On the other hand, inappropriate ECM remodeling also interacts with unresolved inflammation and insufficient angiogenic potential to promote abnormal adipose tissue function and metabolic disturbance [55]. Our research and previous study [26] have found that bariatric surgery relieves the inappropriate ECM remodeling in AT. However, it is not clear whether the appropriate ECM remodeling following RYGB was associated with alleviate metabolic dysfunction. As our study showed, the reduction of ECM accumulation(reduced level of COL3A1) and cross-linking(reduced level of LOX and LOXL1), and the increase of ECM dagradation(primarily the increased level of MMP2) induced by RYGB were positively correlated with the improvement of IR based on HOMA-IR evaluation following RYGB. The current study provides an understanding on the involvement of the appropriate ECM remodeling of scAT in metabolic dysfunction improvement by bariatric surgery.

The current study has the following strengths. First, this study controlled the confounding factors that many previous studies have neglected. The inclusion of a sham treatment group who had the similar characteristics to the intervention group could effectively control the possible influence of irrelevant variables on the scAT transcriptome. Second, bioinformatics analysis was employed to provide a more complete picture of key molecular signatures in scAT following RYGB than study of single gene. Also, although the microarray platform was already published, we carried out a new analysis to this transcriptome data and drew a conclusion from a bioinformatics perspective. Last, the validation experiment was employed in our study because simple bioinformatics analysis results will be affected by arithmetic, parameters and other factors. Our validation experiment further confirmed that the above factors have minimal to no effects on the reliability of the result.

There are some limitations to this study. First, the microarray data provided by Guijarro et al. [30] is relatively old as the original microarray article was published > 10 years ago. However, the current study provide a further biological validation of the transcriptome data. The bioinformatics findings of this transcriptome data were well verified in our animal model. Therefore, the quality of transcriptome data is relatively reliable. Second, RT-PCR and Masson's Trichrome staining for detecting ECM alterations are not comprehensive enough owing to the absence of protein level detection. But Liu's study [26] examined the ECM at protein level by immunohistochemistry, which provided some evidences for our research. Third, the sample size of our animal model is relatively small. In the future, a larger sample size is needed to confirm these findings.

5. Conclusion

By comparing the transcriptional characteristics of subcutaneous fat samples between RYGB and sham-operated control rats and verification the bioinformatics findings in experimental rat model, we discovered that appropriate ECM remodeling - primarily ECM accumulation, cross-linking reduction, and ECM degradation increase -, was the key molecular target in scAT following RYGB. These findings were partly supported by human studies. It is critical to better delineate the mechanisms leading to appropriate ECM remodeling of scAT by RYGB at the cellular level, and to determine the impact of scAT remodeling on metabolic improvements.

Conflict of interest statement

The authors declare that there are no conflicts of interest.

Author contribution

Xiangjun Chen designed the study, conducted the data analysis, and wrote the manuscript; Lilin Gong assisted with study design and data analysis; Qifu Li assisted with study design and revised the manuscript; Jinbo Hu contributed to statistical analyses; Xiurong Liu, Yao Wang and Jie Bai assisted with the data collection; Xi Ran contributed to figures; Jinshan Wu and Qian Ge contributed to the writing of the manuscript; Rong Li, Xiaoqiu Xiao, Jun Zhang, and Xi Li edited the manuscript; Zhihong Wang designed the study and revised the manuscript. Zhihong Wang is the guarantor of the work. She has full access to all the data in the study and takes responsibility for the integrity of the data and the accuracy of the data analysis. All Authors read and approved the final manuscript.

Acknowledgements

We sincerely thank participants of this study. Special thanks to prof. Longke Ran from Department of Bioinformatics, Chongqing Medical University, for helping us with bioinformatics analysis. Thanks to Laurent I from Department of Endocrinology, First Affiliated Hospital of Chongqing Medical University, and Shichao Han from College of Letters and Science, University of California, Berkeley, for helping us revising the English language.

This work was supported by the National Natural Science Foundation of China, China [grant number 81800757]; the Young and Middle-age High-end Medical Reserve Personnel Training Plan

Foundation of Chongqing, China [grant number YuWeiRen [2015]49]; the National Key Clinical Specialties Construction Program of China, China [grant number [2011]170]; the Fundamental Science and Advanced Technology Research of Chongqing, China [grant number cstc2015jcyjBX0096]; and the Natural Science Foundation of Chongqing, China [grant number CSTC2012jjA10040].

Appendix A. Supplementary data

Supplementary data to this article can be found online at https://doi.org/10.1016/j.lfs.2018.12.051.

References

[1] G. Danaei, M.M. Finucane, Y. Lu, et al., National, regional, and global trends in fasting plasma glucose and diabetes prevalence since 1980: systematic analysis of health examination surveys and epidemiological studies with 370 country-years and 2.7 million participants, Lancet 378 (2011) 31–40, https://doi.org/10.1016/S0140-6736(11)60679-X.

[2] D.W. Haslam, W.P. James, Obesity, Lancet 366 (2005) 1197–1209, https://doi.org/10.1016/S0140-6736(05)67483-1.

[3] P.R. Schauer, S.R. Kashyap, K. Wolski, et al., Bariatric surgery versus intensive medical therapy in obese patients with diabetes, N. Engl. J. Med. 366 (2012) 1567–1576, https://doi.org/10.1056/NEJMoa1200225.

[4] S.R. Kashyap, D.L. Bhatt, K. Wolski, et al., Metabolic effects of bariatric surgery in patients with moderate obesity and type 2 diabetes: analysis of a randomized control trial comparing surgery with intensive medical treatment, Diabetes Care 36 (2013) 2175–2182, https://doi.org/10.2337/dc12-1596.

[5] A. Cotillard, C. Poitou, A. Torcivia, et al., Adipocyte size threshold matters: link with risk of type 2 diabetes and improved insulin resistance after gastric bypass, J. Clin. Endocrinol. Metab. 99 (2014) E1466–E1470, https://doi.org/10.1210/jc.2014-1074.

[6] D.P. Andersson, H.D. Eriksson, A. Thorell, et al., Changes in subcutaneous fat cell volume and insulin sensitivity after weight loss, Diabetes Care 37 (2014) 1831–1836, https://doi.org/10.2337/dc13-2395.

[7] H.E. Bays, B. Laferrere, J. Dixon, et al., Adiposopathy and bariatric surgery: is 'sick fat' a surgical disease? Int. J. Clin. Pract. 63 (2009) 1285–1300, https://doi.org/10.1111/j.1742-1241.2009.02151.x.

[8] S. Appachi, K.R. Kelly, P.R. Schauer, et al., Reduced cardiovascular risk following bariatric surgeries is related to a partial recovery from "adiposopathy", Obes. Surg. 21 (2011) 1928–1936, https://doi.org/10.1007/s11695-011-0447-5.

[9] M. Abdennour, S. Reggio, N.G. Le, et al., Association of adipose tissue and liver fibrosis with tissue stiffness in morbid obesity: links with diabetes and BMI loss after gastric bypass, J. Clin. Endocrinol. Metab. 99 (2014) 898–907, https://doi.org/10.1210/jc.2013-3253.

[10] Y.J. Lee, Y.S. Heo, H.S. Park, et al., Serum SPARC and matrix metalloproteinase-2 and metalloproteinase-9 concentrations after bariatric surgery in obese adults, Obes. Surg. 24 (2014) 604–610, https://doi.org/10.1007/s11695-013-1111-z.

[11] J. Chen, Z. Pamuklar, A. Spagnoli, A. Torquati, Serum leptin levels are inversely correlated with omental gene expression of adiponectin and markedly decreased after gastric bypass surgery, Surg. Endosc. 26 (2012) 1476–1480, https://doi.org/10.1007/s00464-011-2059-5.

[12] M.J. Kim, P. Marchand, C. Henegar, et al., Fate and complex pathogenic effects of dioxins and polychlorinated biphenyls in obese subjects before and after drastic weight loss, Environ. Health Perspect. 119 (2011) 377–383, https://doi.org/10.1289/ehp.1002848.

[13] A. Tschoner, W. Sturm, J. Engl, et al., Plasminogen activator inhibitor 1 and visceral obesity during pronounced weight loss after bariatric surgery, Nutr. Metab. Cardiovasc. Dis. 22 (2012) 340–346, https://doi.org/10.1016/j.numecd.2010.07.009.

[14] A. Oberbach, N. Schlichting, J. Neuhaus, et al., Establishing of areliable multiple reaction monitoring-based method for the quantification of obesity associated co-morbidities in serum and adipose 806 Bariatric surgery and adipose tissue requires intensive clinical validation, J. Proteome Res. 13 (2014) 5784–5800, https://doi.org/10.1021/pr500722k.

[15] X. Terra, T. Auguet, I. Quesada, et al., Increased levels and adipose tissue expression of visfatin in morbidly obese women: the relationship with pro-inflammatory cytokines, Clin. Endocrinol. 77 (2012) 691–698, https://doi.org/10.1111/j.1365-2265.2011.04327.x.

[16] X. Terra, T. Auguet, E. Guiu-Jurado, et al., Long-term changes in leptin, chemerin and ghrelin levels following different bariatric surgery procedures: Roux-en-Y gastric bypass and sleeve gastrectomy, Obes. Surg. 23 (2013) 1790–1798, https://doi.org/10.1007/s11695-013-1033-9.

[17] R. Cancello, C. Henegar, N. Viguerie, S. Taleb, C. Poitou, C. Rouault, et al., Reduction of macrophage infiltration and chemoattractant gene expression changes in white adipose tissue of morbidly obese subjects after surgery-induced weight loss, Diabetes 54 (2005) 2277–2286, https://doi.org/10.2337/diabetes.54.8.2277.

[18] R. Chakaroun, M. Raschpichler, N. Kloting, A. Oberbach, G. Flehmig, M. Kern, et al., Effects of weight loss and exercise on chemerin serum concentrations and adipose tissue expression in human obesity, Metabolism 61 (2012) 706–714, https://doi.org/10.1016/j.metabol.2011.10.008.

[19] D. Bradley, C. Conte, B. Mittendorfer, J.C. Eagon, J.E. Varela, E. Fabbrini, et al., Gastric bypass and banding equally improve insulin sensitivity and beta cell function, J. Clin. Invest. 122 (2012) 4667–4674, https://doi.org/10.1172/JCI64895.

[20] A.R. Moschen, C. Molnar, S. Geiger, I. Graziadei, C.F. Ebenbichler, H. Weiss, et al., Anti-inflammatory effects of excessive weight loss: potent suppression of adipose interleukin 6 and tumour necrosis factor alpha expression, Gut 59 (2010) 1259–1264, https://doi.org/10.1136/gut.2010.214577.

[21] V.G. Sams, C. Blackledge, N. Wijayatunga, P. Barlow, M. Mancini, G. Mancini, et al., Effect of bariatric surgery on systemic and adipose tissue inflammation, Surg. Endosc. 30 (2015) 3499–3504, https://doi.org/10.1007/s00464-015-4638-3.

[22] T.B. Curry, S.K. Roberts, R. Basu, et al., Gastric bypass surgery is associated with near-normal insulin suppression of lipolysis in nondiabetic individuals, Am. J. Physiol. Endocrinol. Metab. 300 (2011) E746–E751, https://doi.org/10.1152/ajpendo.00596.2010.

[23] F. Soriguer, S. Garcia-Serrano, J.M. Garcia-Almeida, et al., Changes in the serum composition of free-fatty acids during an intravenous glucose tolerance test, Obesity (SilverSpring) 17 (2009) 10–15, https://doi.org/10.1038/oby.2008.475.

[24] M. Hansen, M.T. Lund, E. Gregers, et al., Adipose tissue mitochondrial respiration and lipolysis before and after a weight loss by diet and RYGB, Obesity 23 (2015) 2022–2029, https://doi.org/10.1002/oby.21223.

[25] C.M. Kusminski, P.E. Bickel, P.E. Scherer, Targeting adipose tissue in the treatment of obesity-associated diabetes, Nat. Rev. Drug Discov. 15 (2016) 639–660, https://doi.org/10.1038/nrd.2016.75.

[26] Y. Liu, J. Aron-Wisnewsky, G. Marcelin, et al., Accumulation and changes in composition of collagens in subcutaneous adipose tissue after bariatric surgery, J. Clin. Endocrinol. Metab. 101 (2016) 293–304, https://doi.org/10.1210/jc.2015-3348.

[27] C. Henegar, J. Tordjman, V. Achard, et al., Adipose tissue transcriptomic signature highlights the pathological relevance of extracellular matrix in human obesity, Genome Biol. 9 (2008) R14, https://doi.org/10.1186/gb-2008-9-1-r14.

[28] R. Cancello, A. Zulian, D. Gentilini, et al., Permanence of molecular features of obesity in subcutaneous adipose tissue of ex-obese subjects, Int. J. Obes. 37 (2013) 867–873, https://doi.org/10.1038/ijo.2013.7.

[29] P. Sedgwick, Before and after study designs, BMJ 8 (349) (2014) g5074, https://doi.org/10.1136/bmj.g5074.

[30] A. Guijarro, S. Suzuki, C. Chen, et al., Characterization of weight loss and weight regain mechanisms after Roux-en-Y gastric bypass in rats, Am. J. Phys. Regul. Integr. Comp. Phys. 293 (2007) R1474–R1489, https://doi.org/10.1152/ajpregu.00171.2007.

[31] L. Gautier, L. Cope, B.M. Bolstad, R.A. Irizarry, Affy-analysis of Affymetrix GeneChip data at the probe level, Bioinformatics 20 (2004) 307–315, https://doi.org/10.1093/bioinformatics/btg405.

[32] G.K. Smyth, Limma: linear models for microarray data, Bioinformatics and Computational Biology Solutions Using R and Bioconductor, Springer, New York, 2005, pp. 397–420.

[33] Y. Tang, M. Li, J. Wang, et al., CytoNCA: a cytoscape plugin for centrality analysis and evaluation of protein interaction networks, Biosystems 127 (2015) 67–72, https://doi.org/10.1016/j.biosystems.2014.11.005.

[34] H. Jeong, S.P. Mason, A.L. Barabási, Z.N. Oltvai, Lethality and centrality in protein networks, Nature 411 (2001) 41–42, https://doi.org/10.1038/35075138.

[35] K.I. Goh, E. Oh, B. Kahng, D. Kim, Betweenness centrality correlation in social networks, Phys. Rev. E Stat. Nonlinear Soft Matter Phys. 67 (2003) 017101, , https://doi.org/10.1103/PhysRevE.67.017101.

[36] E. Estrada, J.A. Rodríguez-Velázquez, Subgraph centrality in complex networks, Phys. Rev. E Stat. Nonlinear Soft Matter Phys. 71 (2005) 056103, , https://doi.org/10.1103/PhysRevE.71.056103.

[37] S. Zhang, W. Guo, J. Wu, et al., Increased β-cell mass in obese rats after gastric bypass: a potential mechanism for improving glycemic control, Med. Sci. Monit. 23 (2017) 2151–2158, https://doi.org/10.12659/MSM.902230.

[38] S. Mu, J. Liu, W. Guo, et al., Roux-en-Y gastric bypass improves hepatic glucose metabolism involving down-regulation of protein tyrosine phosphatase 1B in obese rats, Obes. Facts 10 (2017) 191–206, https://doi.org/10.1159/000470912.

[39] D.R. Matthews, J.P. Hosker, A.S. Rudenski, et al., Homeostasis model assessment: insulin resistance and beta-cell function from fasting plasma glucose and insulin concentrations in man, Diabetologia 28 (1985) 412–419.

[40] S.N. Dankel, J. Svärd, S. Matthä, et al., COL6A3 expression in adipocytes associates with insulin resistance and depends on PPARγ and adipocyte size, Obesity (Silver Spring) 22 (2014) 1807–1813, https://doi.org/10.1002/oby.20758.

[41] M. Spencer, R. Unal, B. Zhu, et al., Adipose tissue extracellular matrix and vascular abnormalities in obesity and insulin resistance, J. Clin. Endocrinol. Metab. 96 (2011) E1990–E1998, https://doi.org/10.1210/jc.2011-1567.

[42] T. Khan, E.S. Muise, P. Iyengar, et al., Metabolic dysregulation and adipose tissue fibrosis: role of collagen VI, Mol. Cell. Biol. 29 (2009) 1575–1591, https://doi.org/10.1128/MCB.01300-08.

[43] N. Halberg, T. Khan, M.E. Trujillo, et al., Hypoxia-inducible factor 1alpha induces fibrosis and insulin resistance in white adipose tissue, Mol. Cell. Biol. 29 (2009) 4467–4483, https://doi.org/10.1128/MCB.00192-09.

[44] T.A. Wynn, Common and unique mechanisms regulate fibrosis in various fibroproliferative diseases, J. Clin. Invest. 117 (2007) 524–529, https://doi.org/10.1172/JCI31487.

[45] A. Graja, F. Garcia-Carrizo, A.M. Jank, et al., Loss of periostin occurs in aging adipose tissue of mice and its genetic ablation impairs adipose tissue lipid metabolism, Aging Cell 17 (2018) e12810, , https://doi.org/10.1111/acel.12810.

[46] K. Sun, J. Tordjman, K. Clément, P.E. Scherer, Fibrosis and adipose tissue dysfunction, Cell Metab. 18 (2013) 470–477, https://doi.org/10.1016/j.cmet.2013.06.016.

[47] P. Trayhurn, J.H. Beattie, Physiological role of adipose tissue: white adipose tissue as an endocrine and secretory organ, Proc. Nutr. Soc. 60 (2001) 329–339, https://doi.org/10.1079/PNS200194.
[48] X. Fu, L. Fang, H. Li, et al., Adipose tissue extract enhances skin wound healing, Wound Repair Regen. 15 (2007) 540–548, https://doi.org/10.1111/j.1524-475X.2007.00262.x.
[49] Xiong Qian, Weidong Lin, Wanli Jiang, et al., Changes of mature adipocytes after incision injury of subcutaneous adipose tissue, J. Tongji Univ. (Med. Sci.) 33 (2012) 5–10, https://doi.org/10.3969/j.issn1008-0392.2012.05.002.
[50] K. Chabot, M.S. Gauthier, P.Y. Garneau, R. Rabasa-Lhoret, Evolution of subcutaneous adipose tissue fibrosis after bariatric surgery, Diabetes Metab. 43 (2017) 125–133, https://doi.org/10.1016/j.diabet.2016.10.004.
[51] D.M. Mutch, J. Tordjman, V. Pelloux, et al., Needle and surgical biopsy techniques differentially affect adipose tissue gene expression profiles, Am. J. Clin. Nutr. 89 (2009) 51–57, https://doi.org/10.3945/ajcn.2008.26802.
[52] R. Agarwal, P. Agarwal, Targeting extracellular matrix remodeling in disease: could resveratrol be a potential candidate? Exp. Biol. Med. (Maywood) 242 (2017) 374–383, https://doi.org/10.1177/1535370216675065.
[53] M.A. Karsdal, T. Manon-Jensen, F. Genovese, et al., Novel insights into the function and dynamics of extracellular matrix in liver fibrosis, Am. J. Physiol. Gastrointest. Liver Physiol. 308 (2015) G807–G830, https://doi.org/10.1152/ajpgi.00447.2014.
[54] M.C. Lampi, C.A. Reinhart-King, Targeting extracellular matrix stiffness to attenuate disease: from molecular mechanisms to clinical trials, Sci. Transl. Med. 10 (2018), https://doi.org/10.1126/scitranslmed.aao0475.
[55] C. Crewe, Y.A. An, P.E. Scherer, The ominous triad of adipose tissue dysfunction: inflammation, fibrosis, and impaired angiogenesis, J. Clin. Invest. 127 (2017) 74–82, https://doi.org/10.1172/JCI88883.